

Seminar Nasional Tahunan Teknik Mesin (SNTTM) VIII

Universitas Diponegoro, Semarang 11-12 Agustus 2009

M3-013 Mechanical Properties and Corrosion Behaviour of Spiral Welded API 5L X-52 Steel Line Pipe

Mochammad Noer Iman^a, Nur Subeki^b and Jarot Wijayanto^c

^a Department of Mechanical and Industrial Engineering, Gadjah Mada University, Yogyakarta

^b Department of Mechanical Engineering, Muhammadiyah University of Malang, Malang

^c Department of Mechanical Engineering, IST Akrprind, Yogyakarta

Phone/Fax : (0274)521673, E-mail : ilman_noer@ugm.ac.id

ABSTRACT

Spiral welded API 5L X-52 steel line pipes have been in service for many years as oil and gas transmission pipes. Such pipes are usually produced by forming hot-rolled coil (HRC) steels into tubular products and welding is performed along spirally joining lines using submerged arc welding (SAW) process. The weld metal used for oil and gas line pipes must fulfil the more stringent requirements such as high strength, good impact toughness and high corrosion resistance. The present investigation aims to study mechanical properties and corrosion behaviour of submerged arc spiral welded API 5L X-52 steel line pipe.

The spiral welded steel API X-52 line pipes were produced using submerged arc welding with the filler of EM12K and flux of OK10,71. Welding parameters, i.e., current, voltage and heat input were 825 A, 35 volt and 2.1 kJ/mm respectively. Subsequently, a sequence of experiments were carried out including microstructural examination, hardness and tensile tests, V-Charpy notch impact test and corrosion test. The corrosion rate was measured using three electrode potential method with saturated calomel (Hg_2Cl_2) electrode (SCE) as the standard electrode whereas the auxiliary electrode was platinum.

Results show that microstructure of submerged arc weld metal for spiral welded steel API X-52 line pipes is composed of acicular ferrite as the dominant phase when filler, flux and welding parameters are properly selected and this type of microstructure seems to give high strength (ultimate strength of 563 MPa and yield stress of 488) and good impact toughness with the ductile-brittle transition temperature of 0 °C.

Keywords: spiral welded pipe, acicular ferrite and mechanical properties

1. Introduction

The oil and gas related industries employ pipelines as the primary mode for transporting gas, crude oil and various petroleum products. For economic reasons, oil or gas pipelines are made of carbon-manganese steels or high strength low alloy (HSLA) steels [1]. In recent years, spiral welded pipes have

Seminar Nasional Tahunan Teknik Mesin (SNTTM) VIII

Universitas Diponegoro, Semarang 11-12 Agustus 2009

been developed because they offer cost benefit over UOE pipes but the acceptance of these pipes for oil and gas applications is markedly varied. Advances made in welding manufacturing techniques enable spiral welded pipes such as API X-52 line pipe to be fabricated using submerged arc welding (SAW) technique with better quality.

Weld Metal Microstructure and Mechanical Properties

Weld metal for oil and gas line pipes must meet the more stringent requirements, i.e. ultimate strength up to 500 MPa and impact toughness of 100 J at 0 °C. These levels of mechanical properties are usually related to particular weld metal microstructure that is acicular ferrite [2].

In steel weld metals, the carbon content is maintained low, typically between 0.05 to 0.1 wt% to maintain good weldability [3,4] and the weld metal microstructure is usually composed of two or more phases arranged in order of decreasing transformation [5] as follows :

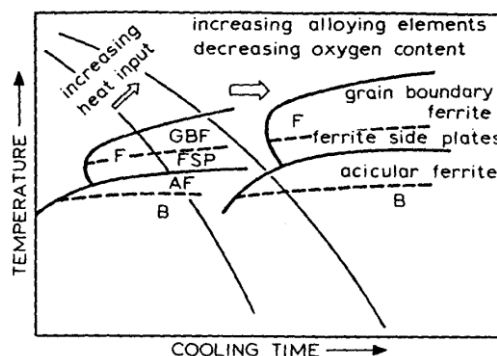
1. Grain boundary ferrite (GF) forms between 1000 to 650 °C at prior austenite grain boundaries
2. Widmanstatten ferrite (WF) forms between 750 to 650 °C emanating from the prior austenite grains
3. Acicular ferrite (AF) forms below 650 °C within the prior austenite grains
4. A lath structure known as bainite (B) forms at 500 °C
5. Microconstituents : martensite, retained austenite and carbide (MAC)

Of these microstructure, acicular ferrite is desirable since it provides high strength via the Hall-Petch relationship and gives high value of impact toughness due to its fine interlocking grains typically 1-3 μm separated by high angle grain boundaries [6]. According to the Hall-Petch equation, the strength of metals is inversely proportional to the square root of grain size :

$$\sigma_y = \sigma_o + kd^{-1/2} \quad (1)$$

where σ_y is yield stress, σ_o is friction stress, k is strengthening coefficient and d is grain size. Hence, according to the equation above, finer acicular ferrite would improve strength of steel weld metals.

It has been known that factors affecting acicular formation include chemical compositions of filler, base metal and flux, heat input and cooling rate [7] and this can be clearly understood using continuous cooling transformation (CCT) diagram in Fig.1.



Seminar Nasional Tahunan Teknik Mesin (SNTTM) VIII

Universitas Diponegoro, Semarang 11-12 Agustus 2009

Figure 1. CCT diagram for steel weld metal [7]

Referring to Fig.1, it can be seen that high input tends to form high transformation temperature products, grain boundary ferrite ferrite side plates whereas very low heat input promotes bainitic microstructure. Increasing alloying elements moves the CCT diagram to the longer time in contrast to oxygen effect. Acicular ferrite tends to form when the amount of oxygen content is in the range of 200-300 ppm with the cooling rate of 5-30 °C/s [8].

Corrosion Resistance

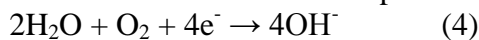
API 5L X-52 steel line pipes are usually used for transporting crude oil mixed with gas and water. Internal corrosion mechanisms in line pipes have been proposed by Palmer and King [1]. As the crude oil velocity is low then the flow pattern is stratified where the gas and liquid completely segregate from each other and water layer forms in oil pipelines. In such a case as this, internal corrosion may occur at the inner surface of the steel pipes according to the anodic reaction as follows :



In sweet corrosion, carbon dioxide is dissolved in water resulting in ions H^+ which subsequently consume the electrons from anode according to the reaction :



In the case of aeration solution with pH of neutral or basic, the cathodic reaction in Eq.(3) becomes :



When this oxidation-reduction reaction occurs then the pipeline surface is corroded forming reddish-brown oxide deposits.

2. Experimental

Materials

API 5L X-52 Base Metal

Material for line pipes was HRC steel specified as API 5L X-52 and the composition is given in Table 1.

Consumables

Consumables used were filler of EM12K and a basic type flux, namely OK 10,71 was selected with their chemical compositions are given in Table 2 and 3 respectively.

Table 1. Chemical composition of HRC steel specified as API 5L X-52

C	Mn	Si	P	S	Nb	V	Ti	Mo	Ni	Cu	Al
0.08	0.9	0.05	0.02	0.01	0.01	0.13	0.07	0.07	0.02	0.13	0.03
					2	3	9		4	1	3

Seminar Nasional Tahunan Teknik Mesin (SNTTM) VIII

Universitas Diponegoro, Semarang 11-12 Agustus 2009

Table 2. Chemical composition of filler EM12K

C	Mn	Si	P	S	Cr	Ni	Mo	Cu
0.11	1.09	0.29	0.009	0.011	0.03	0.02	0.01	0.12

Table 3. Chemical composition of flux OK 10,71

Al ₂ O ₃	SiO ₃	MgO	CaO	MnO	ZrO ₂	TiO	Na ₂ O	K ₂ O	Fe	F	S	P
2-26	18-22	15-19	11-15	6-10	4-7	2-5	1-3	1	1-3	8	<0.03	<0.03

Submerged Arc Welds

The spirally welded pipe was made by wounding the plate spirally forming the pipe and at the same time, spirally internal and external seams were welded using submerged arc welding as shown in Fig. 2.

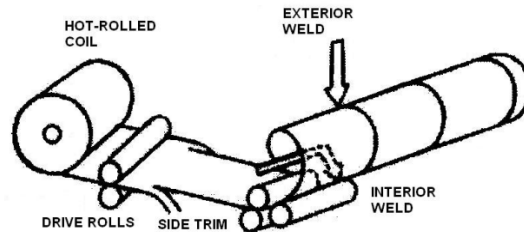


Figure 2. Spiral welded pipe

Welding parameters, i.e., current, voltage and heat input were 825 A, 35 volt and 2.1 kJ/mm respectively.

Microstructure

Microstructural examination was performed using an optical microscope and the samples were prepared using standard preparation techniques including grinding, polishing and etching using natal (2% HNO₃ + 98 propanol).

Hardness

The hardness distribution regions along weld metal, HAZ and base metal were carried out using Vickers microhardness.

Tensile test

Tensile test was conducted using all weld metal specimen where the specimen taken from the weld fusion zone as shown in Fig.3. Specimen were prepared using STP 601 standard.

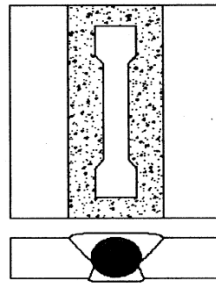


Figure 3. Tensile test specimen

V-Charpy Impact Test

Toughness of weld metal, HAZ and base metal were carried out with the V-Charpy notches parallel to weld line (0°) as shown in Fig. 4.

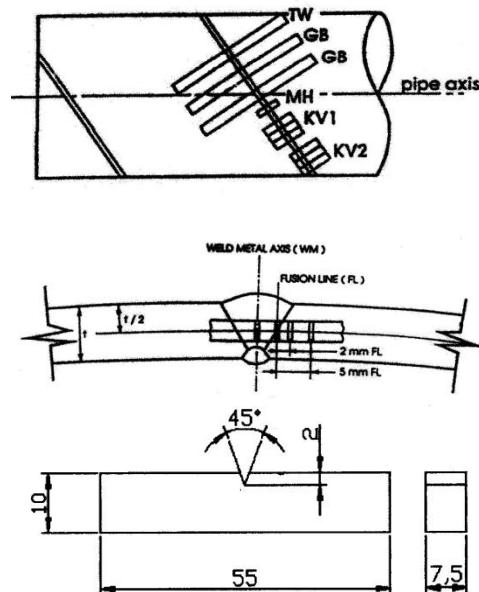


Figure 4. Specimen for impact test

Corrosion in Crude Oil Water

Electrochemical test was conducted using a three-electrode cell with the reference electrode of saturated calomel (Hg_2Cl_2) electrode (SCE) whereas the auxiliary electrode was platinum. The corrosion test was performed in water taken from crude oil.

3. Results And Discussion

Chemical composition

Chemical composition of the weld metal is shown in Table 4. This weld metal composition is resulted from mixture of filler, flux and base metal compositions.

Microstructure

Figure 5 shows macrostructure of spirally submerged arc steel API X-52 weld joints. This type of weld joint is composed of outer weld and inner welds, heat affected zone (HAZ), reheated zone (RHZ) and base metal whereas microstructures present in these regions are shown in Fig.6(a)-(d).

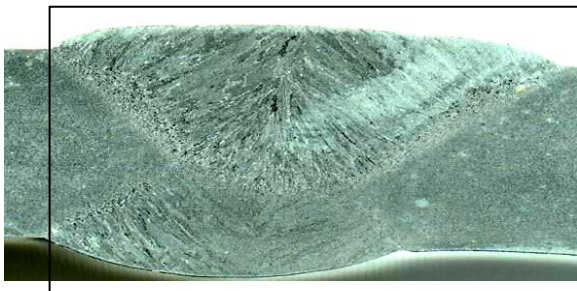


Figure 5. Macrostructures of weldments

Microstructure of the weld metal as shown Fig.6(a) is characterized by the presence of acicular ferrite as the dominant phase which nucleates intragranularly within columnar structures of grain boundary ferrite. A small amount of Widmanstatten ferrite is also observed emanating from the grain boundary ferrite.

Heat affected zone (HAZ) consists of coarse grained (CG) and fine grained (FG) regions as seen in Fig. 6(b) and (c) respectively. The coarse grained (CG) is the region adjacent to the weld metal where the temperature during welding is high, typically above $1100\text{ }^\circ\text{C}$ [4,9] but lower than its melting temperature, hence leading to austenite grain growth. Subsequently, these large austenite grains tend to transform to bainite during cooling. The coarse grained (CG) is the region slightly far from the weld metal where its temperature during welding is lower than $1100\text{ }^\circ\text{C}$ and the nucleation of austenite takes place without grain growth. During cooling, this fine grained austenite transforms to fine ferrite and pearlite grains.

Figure 6(d) shows base metal microstructure consisting of fine ferrite and pearlite which elongate parallel to the rolling direction. This typical microstructure is the product of thermomechanical controlled processing (TMCP).

Seminar Nasional Tahunan Teknik Mesin (SNTTM) VIII

Universitas Diponegoro, Semarang 11-12 Agustus 2009

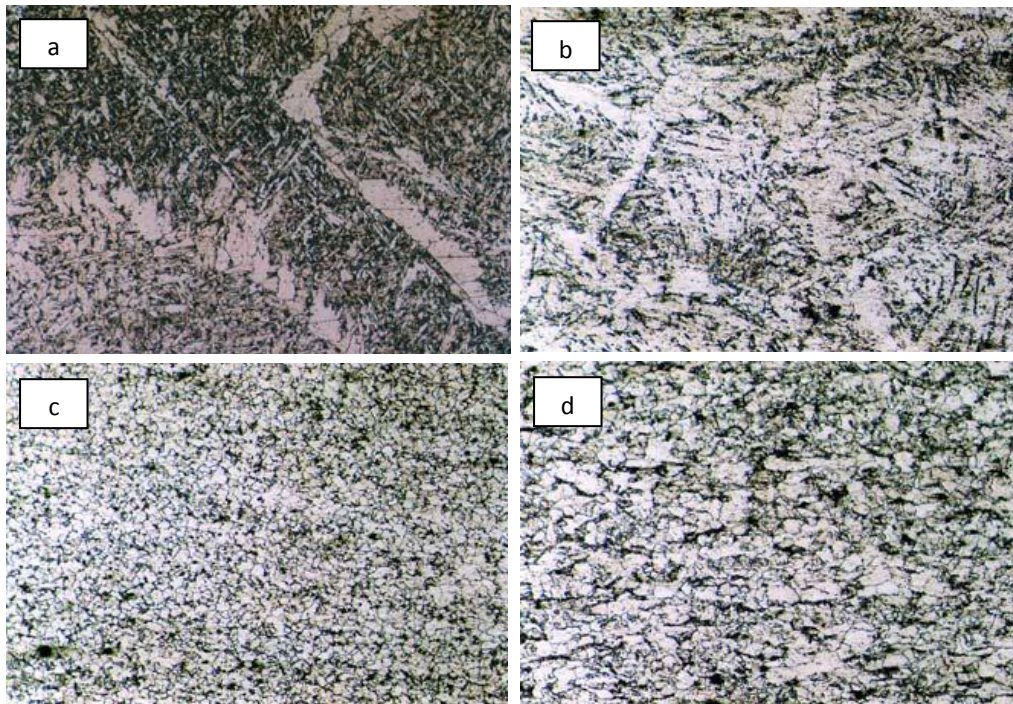


Figure 6. Microstructure of (a) weld metal, (b) coarse grained HAZ, (c) fine grained HAZ and (d) base metal

Table 4. Wed metal composition (wt %)

C	Mn	Si	P	S	Mo	Ni	Al	Co	Cu	Nb	Ti	V	W
0,0	0,9	0.0	0,0	0,0	0,0	0,0	0,0	0,0	0,2	0,0	0,0	0,1	0,0
93	67	41	27	05	07	3	21	01	51	12	79	36	12

Hardness

The hardness distribution of weld metal, HAZ and base metal is shown in Fig.7 . It can be seen that the hardness of base metal is around 230 VHN and the lowest hardness is observed at the fine grained (FG) HAZ but sharp increase in the hardness occurs at the coarse grained (CG) HAZ.

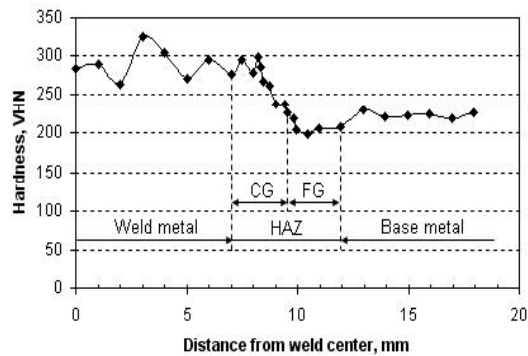


Figure 7. Hardness of weldments

This hardness distribution may be related to the microstructures present in the weldment regions. During welding, recrystallization takes place at the fine grained region resulting in low dislocation density grains with low hardness value whereas at the coarse grained region, large austenite grains tend to form bainite during the austenite to ferrite transformation. The hardness of weld metal is around 300 VHN which is higher than HAZ region and base metal. This may be related to high dislocation density acicular ferrite in weld metal.

Tensile Stresses

The yield and ultimate stresses of base metal and weld metal are shown in Fig.8. It can be seen that the strength of weld metal is slightly similar to that of base metal. Based on the strength, this pipe material can be classified as API 5L X-52.

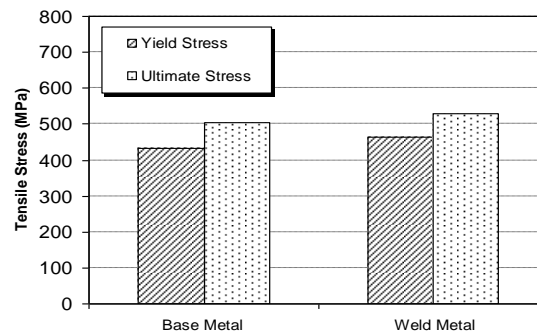


Figure 8. Tensile stresses

Toughness

Results of V-Charpy notch impact tests for the weld metal, HAZ and base metal oriented at 0 and 45° are shown in Fig.9. It seems that the toughness of weld metal is lower than that of the base metal and HAZ for all test temperature. In addition, the brittle-ductile transition temperature of weld metal is around 0 °C whereas the base metal transition temperature is approximately -30 °C. This means that weld joint needs to be paid attention during piping design especially when the pipe is operated at low temperature.

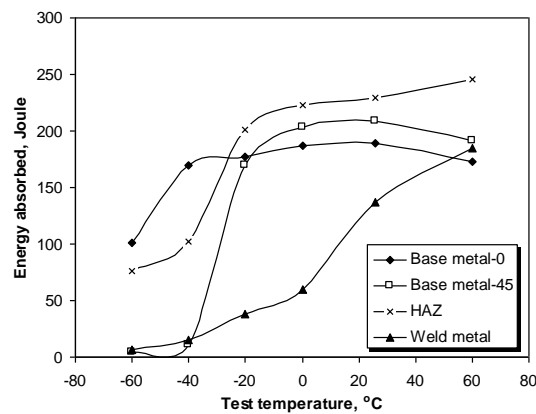
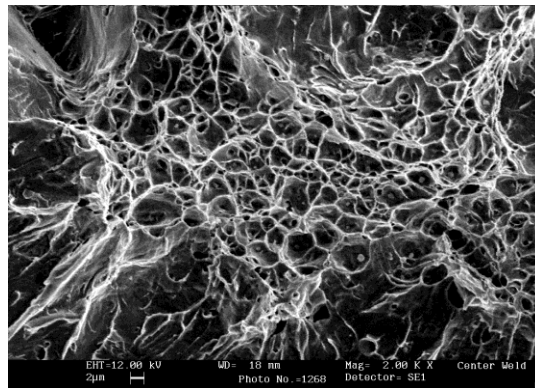
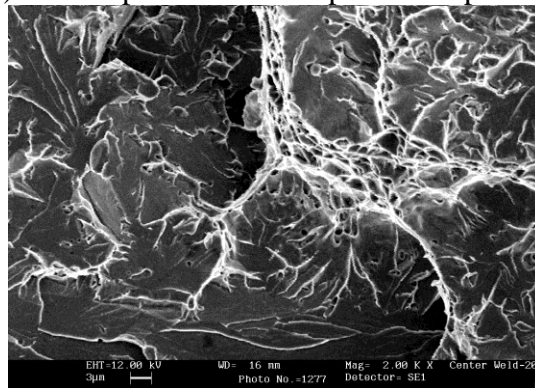


Figure 9. Toughness of weldments

Results of SEM examination on fractured surfaces of the weld metals at atmospheric temperature and -20°C are shown in Fig. 10 (a)-(b). It can be seen that at the atmospheric temperature, the weld metal is relatively ductile as indicated by the presence of dimples which contain inclusions. In contrast, the steel weld metal becomes brittle at low temperature with fractured surface resembles cleavage fracture.



(a) test temperature : atmospheric temperature

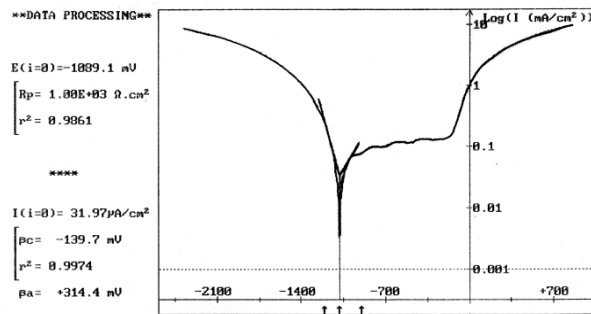
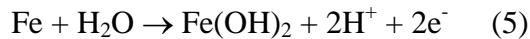


(b) test temperature : -20°C

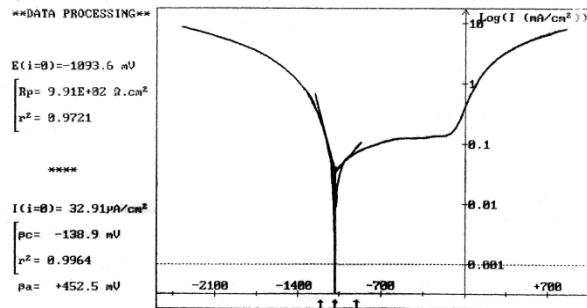
Figure 10. SEM fractured surfaces of weld metal

Corrosion Rate

Figure 11 shows anodic polarization curve for base metal and weld metal in water containing crude oil. Both materials exhibit passivity presumably due to the formation of passive film according to electrochemical reaction [10] such as :



(a) Base metal



(b) Weld metal

Figure 11. Corrosion rate

The corrosion rate (r) can be calculated using the following equations [11] :

$$r = 0,129 \frac{(EW)i}{D} \quad (6)$$

$$EW = (N_{EQ})^{-1} \quad (7)$$

$$N_{EQ} = \sum \left(\frac{f_i}{a_i / n_i} \right) = \sum \left(\frac{f_i n_i}{a_i} \right) \quad (8)$$

Seminar Nasional Tahunan Teknik Mesin (SNTTM) VIII

Universitas Diponegoro, Semarang 11-12 Agustus 2009

where EW : equivalent weight, N_{EQ} : the total number of equivalent, and f_i , n_i and a_i are mass fraction, electrons exchanged and atomic weight respectively. Results of corrosion rate tests are given in Table 5.

Table 5. Corrosion rate

Material	i_{corr} ($\mu\text{A}/\text{cm}^2$)	mpy	mm/year
Weld metal	32.91	15.27	0.3878
Base metal	31.97	14.57	0.3702

Referring to Table 5, it can be seen that corrosion rate of the weld metal and base metal are in the range of 5-20 mpy (0.1-0.5 mm/year) and this typical corrosion resistance is considered to be good. Of note is that corrosion rate between 1-5 mpy is considered to have excellent corrosion resistance and it is outstanding when the corrosion rate is lower than 1 mpy [12]. This means that spirally welded API 5L steel line pipes need corrosion protection during operation.

Conclusions

The conclusions that can be drawn from this investigation are as follows :

1. Weld metal prepared using filler of EM12K (medium manganese content), and basic type flux OK10,71 gives strength approximately similar to that of API 5L X-52 steel pipe when the welding parameter are properly selected with the weld metal microstructure dominated by acicular ferrite.
2. The ductile to brittle transition temperature of weld metal is higher than that of base metal suggesting that the operating temperature of API 5L X-52 line pipe is based on weld metal transition temperature.
3. Corrosion rates for both API 5L X-52 line pipe and its weld joint are in the range of 5-20 mpy (0.1-0.5 mm/year) and this pipe needs to be protected from corrosion during service.

Acknowledgements

The authors appreciate and acknowledge the research support of PT KHI Pipe Industries.

References

1. Palmer, A.C. and King, R.A., *Subsea pipeline engineering*, PennWell, Oklahoma, USA, 2004
2. Cochrane, R.C. and Keville, B.R., Influence of inclusion morphology on microstructure and toughness of submerged arc weldments, Proceedings of international conference on : steels for line pipe and pipeline fittings, London, 1981.
3. Lancaster, J.F., *Metallurgy of Welding*, Abington Publishing, Cambridge, UK, 1999
4. Easterling, K.E., *Introduction to the Physical Metallurgy of Welding*, Butterworth-Heinemann, London, UK, 1992

Seminar Nasional Tahunan Teknik Mesin (SNTTM) VIII

Universitas Diponegoro, Semarang 11-12 Agustus 2009

5. Abson,D.J. and Pargeter,R.J., *Factors Influencing Strength, Microstructure and Toughness of as Deposited Manual Metal Arc Welds Suitable for C-Mn Steel Fabrications*, International Metal Reviews, Vol.31, No.4, (1986), 141-193
6. Harrison,P.L and Farrar,R.A., *Influence of oxygen-rich inclusions on the $\gamma \rightarrow \alpha$ phase transformation in high strength low alloy (HSLA) steel weld metals*, Journal of Materials Science, vol.16, (1981), 2218-2226
7. Ito,Y and Nakanishi,M., *Study of Charpy impact properties of weld metal with submerged-arc welding*, Sumitomo Search, 15, (1976) 42
8. Thewlis,G., *Proceeding of International Conference on : Welding and performance of pipelines*, Welding Institute, London, UK, Paper No.9, 1986
9. Ramirez,J.E., Michael,S. and Shockley,R., *Properties and sulfide stress cracking resistance of coarse-grained heat affected zones in V-microalloyed X60 steel pipe*, Welding Journal, (2005), 113-123
10. Trethewey,K.R., and Chamberlain,J., *Corrosion for science and engineering*, 2nd ed, Longman Group Ltd, Essex, UK, 1995
11. Jones,D.A., *Principles and prevention of corrosion*, Prentice-Hall,Inc., 2nd ed, New York, USA, 1996
12. Fontana, M.G., *Corrosion Engineering*, McGraw-Hill, 3rd ed., New York, USA, 1986.